WAXD INVESTIGATION OF THE SECOND ORDER RESIDUAL STRESS INTO THREE HIGH ALLOYED STEELS

ION V. POPESCU[1], FLORINA VIOLETA ANGHELINA[1], ION I. PENCEA[2], EUGEN CATALIN SFAT[2]

[1]*Valahia* University Targoviste, Faculty of Sciences and Arts, 18-20 Unirii Av., 130082, Targoviste, Romania
[2]*Politehnica* University of Bucharest, Faculty of Materials Science and Engineering, 313 Splaiul Independentei, 14035, Bucharest, Romania

Abstract: *Mechanical processing like milling, polishing, grinding, etc generate internal residual stresses of the first order (macrostresses) at bulk level and of the second order (σ_{II}) at the crystallite level [1-5]. The paper addresses the σ_{II} depth profiles induced by milling and mechanical polishing in three high alloyed steel grades of AISI 316 types. These grades are used for implants manufacture. The σ_{II} depth profiles were used to select the proper mechanical regime related to steel grade in order to minimize cracks initiation and/or cracks propagation. These researches take part from a large project aimed to improve metallic implant manufacture technology.*

Keywords: *X-ray diffraction, internal residual stresses, high alloyed steel, microstresses..*

1. Introduction

For the critical parts of implants as hip joint head, hip socket etc it is very important that residual stresses σ_{II} induced by mechanical processing to be at minimum level. This is because the crack initiation and/or crack propagation are stimulated by the field of micro-stresses induced by different technological machining. Because the parts technology implies milling and mechanical polishing as successive final stages before introducing them in use we studied the σ_{II} induced by milling and three different polishing regimes. We consider that the σ_{II} depth profiles are much more significant than ordinary σ_{II} surface measurements. So, we evaluated the σ_{II} from the surface to 150 μm depths, step 10 μm, by electrochemical successive layers removal method. The micro-stresses were evaluated from X-ray diffractometric measurements using the standard method [1-3].

From technological view point, the X-ray diffraction measurement of the second order residual stresses using standard method is reliable.

2. Experimental

There were investigated three grades of high alloyed steels whose chemical compositions are given in Table 1.

Table 1. The main composition of the investigated grades

	C	Si	Mn	P	S	Cr	Mo	Ni	Al	Co	Nb	V	W
HAS1	0,041	1,46	1,95	0,015	0,002	17,8	2,31	12,71	0,07	0,11	0,04	0,09	0,26
HAS2	0,048	1,44	1,92	0,016	0,002	16,6	2,34	12,54	0,10	0,23	0,04	0,08	0,47
HAS3	0,037	1,50	1,82	0,018	0,002	18,5	2,32	12,72	0,06	0,10	0,03	0,09	0,21

The microstructure of the HAS grades give an overview of the potential influence factors on σ_{11} measurand as steel cleanness, grain size, grain size homogeneity, degree of grain preferential orientation [7, 8].

Figure 1. The austenitic microstructure of HAS 1 grade. Etching: 1:1/HCl:HNO_3

As could be seen from Figure 1 to Figure 3 the microstructure of the grades are different and their cleanness the same. Though, from WAXD considerations their structure is proper for significant measurement of secondary stresses because the average grain sizes are greater than 20 μm.

The specimens from all above-mentioned steels were cut with 50 x 40 x 10 mm dimensions from raw ingots. One of the two faces of 50 x 40 mm of each parallelipipedron was machined with a "widia" head at a low speed (100 mm/sec) in order to obtain a smooth surface. It was machined in the same conditions nine samples from each of the three steel marks. In the case of mechanical polishing we studied three polishing regimes: low speed polishing (150 rot/min), high speed polishing (1500 rot/min) and high speed-vibration contact polishing (1500 rot/min) (85 Hz). These regimes were performed with a Nematron machine using synthetic diamond powder mesh 400. The distances between the disk center of the polishing machine and samples were about 160 mm. The forces applied on top faces of the samples, during polishing were about 10 N in all cases.

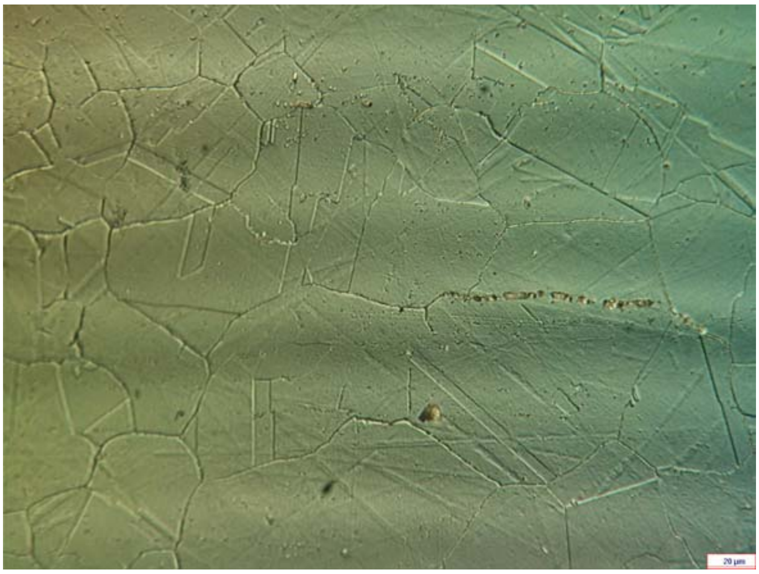

Figure 2. The austenitic microstructure of HAS 2 grade. Etching: 1:1/HCl:HNO_3

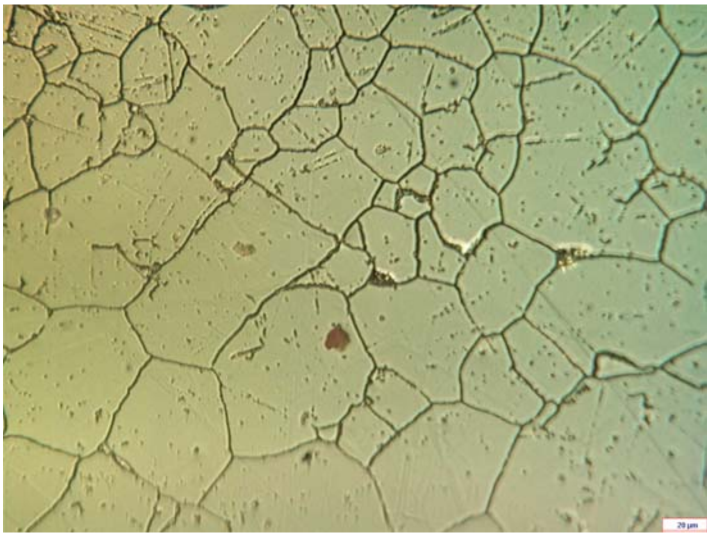

Figure. 3. The austenitic microstructure of HAS 3 grade. Etching: 1:1/HCl:HNO_3

After being polished the samples were cleaned in special devices using alcohol and water. The measurements of stresses were done with a standard DRON3 diffractometer which was up-graded and real time computer assisted. The X-ray tube operated at 40 kV and 35 mA. The $Mo_{K\alpha}$ radiation diffracted by the (211) martensitic planes impinged on a graphite monochromator (004 planes). The WAXD diffractograms given by the HAS grades are quite similar. The common aspect of WAXD diffractogram for all investigated grades is shown in Figure. 4.
The internal residual stresses σ_{11} were evaluated using well-known relation [2, 3, 6]:

$$\sigma_{11} = \left(\frac{-E}{\nu} \right) \cdot \left(B^2 - B_0^2 \right)^{1/2} \left(4tg\theta \right)^{-1} \quad (1)$$

The σ_{11} can be considered as a surface stress state because the $Mo_{K\alpha}$ X-ray depth of radiation penetration is less than 5 μm in such steels.

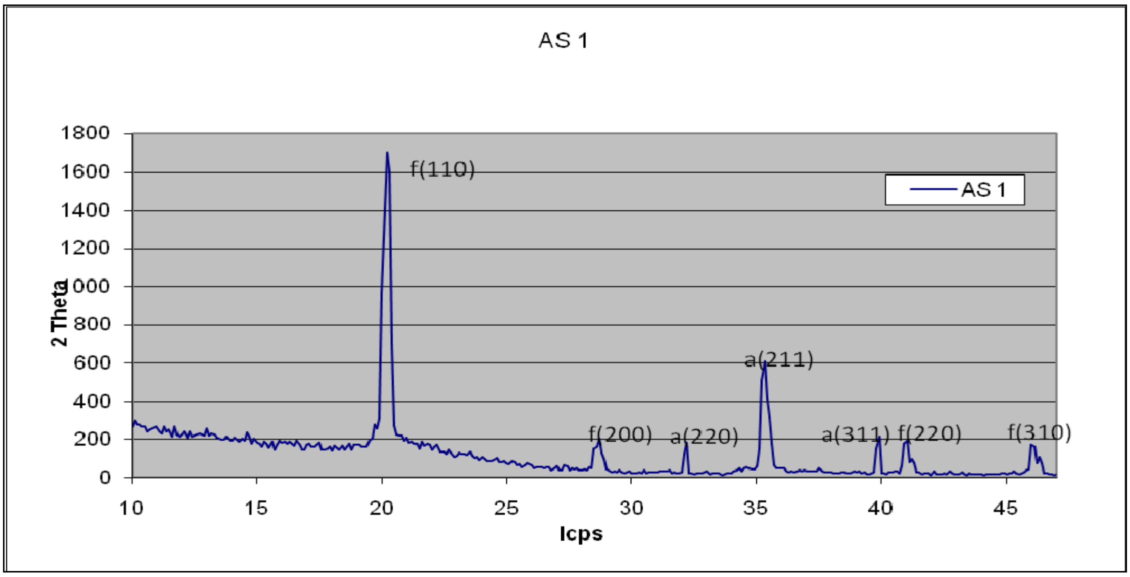

Figure. 4. The WAXD pattern of the HAS 1 grade.

In order to draw the σ_{11} depth profiles induced by mechanical processing in above mentioned steels it was successive removed layers of 10 μm thickness by electro polishing in a Bollman type device. The solution's composition for such steels is (volumetric %): 65 % orthophosphoric acid and 35 % sulphuric acid. The optimal electrical parameters founded for HAS 1, HAS2 and HAS3 are, respectively, tensions: 40; 44; 37 V at current densities of 1.1; 1.25 and 0.95 A/cm^2.

Every ferrite (211) diffraction line was ten times recorded at each depth. The experimental B and B_0 were taken as average values. Previously B and B_0 determination, the (211) lines were subjected to usually corrections (smooth, background, LP, etc) using up-graded DRON 3 software. After these corrections, the lines were fitted with Gauss, Cauchy and Lorentz functions in order to evaluate which kind of B correction is better i.e. $(B^2 - B_0{}^2)^{1/2}$, B-B_0 or other [3--6]. We find out that the (211) lines are better fitted by the Gaussian profiles. That is why we used the relation (1) to calculate σ_{11}. The B and B_0 values were estimated step-by-step, step 10 μm, from the surface to 150 μm depths.

4. Results and discussion

The mechanical parameter (E, υ) of the HAS1, HAS 2 and HAS 3 steels used for σ_{11} calculations were obtained from their ultimate tensile strength data. The E and υ are: S1 (2.1 GPa, 0.29); S2 (2.38 GPa, 0.28); S3 (2.43 GPa, 0.28).

The low speed milling of these steels caused specific plastic deformation of the first surface layers which are associated with positive σ_{11} values. The σ_{11} depth profiles induced by milling of HAS1, HAS 2 and HAS 3 steels are given in Figureure 1. They show that the same milling regime induce different σ_{11} depth distribution in S1, S2 and S3 martensitic steels.

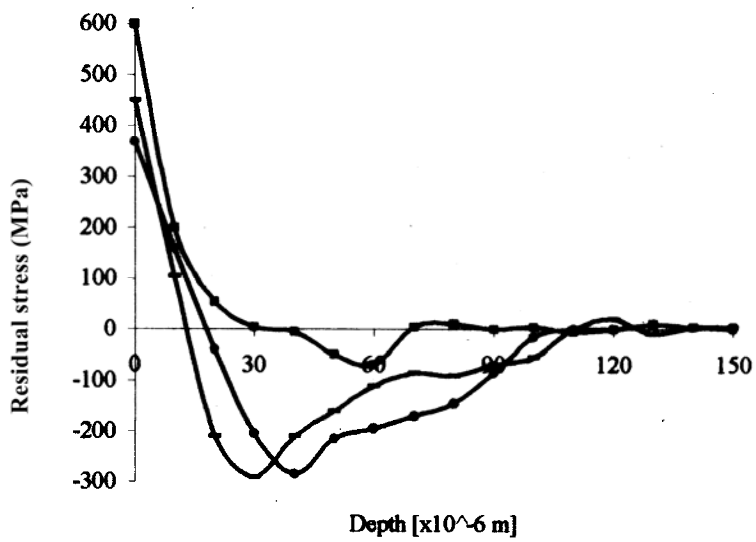

Figure. 5. The residual stresses (σ_{11}) depth profiles induced by machining milling in S1, S2 and S3 steel marks (• - HAS 1; ■ - HAS 2; — - HAS 3)

From Figure 5 it results that at about 20 μm depth the σ_{11} changes its sign and at about 40 μm the compressive microstress reach a maximum intensity. From a 100 μm depth the σ_{11} values attend the equilibrium level.

The residual stresses distributions versus depth in HAS 1, HAS 2 and HAS 3 steels by the above three mentioned mechanical polishing regimes are given in Figures 6, 7 and 8.

As it can be seen from Figure 6 the three σ_{11} profiles of the HAS 1, HAS 2 and HAS 3 polished steels have similar shapes. The surface σ_{11} values ranges between - 400 MPa and - 500 MPa and decreases rapidly below the surface i.e. in the first 15-20 μm depth.

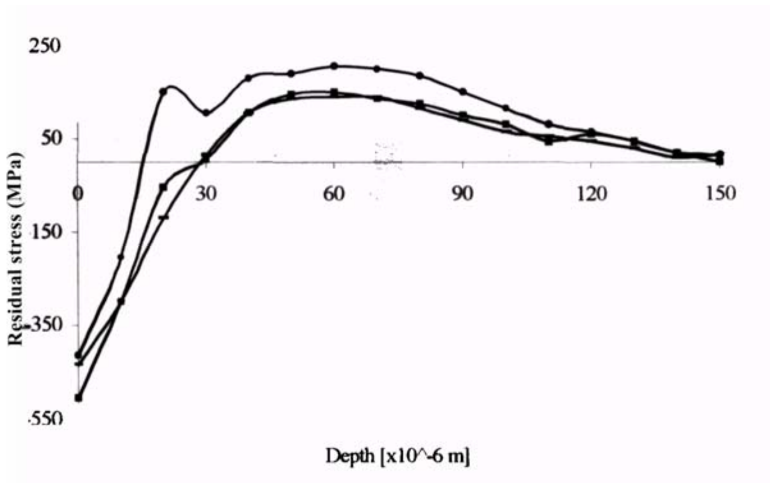

Figure. 6. The residual stresses (σ_{11}) depth profiles by low-speed mechanical polishing in HAS 1, HAS 2 and HAS 3 steel marks (• - S1; ■ - S2; — - S3)

The high-speed polishing regime induced high microstress state in the surface layers ranging between -500 and 650 MPa as it is shown in Figure7.

The σ_{11} profiles in Figure 7 show that the microstresses change their signs at a depth around 50 μm.

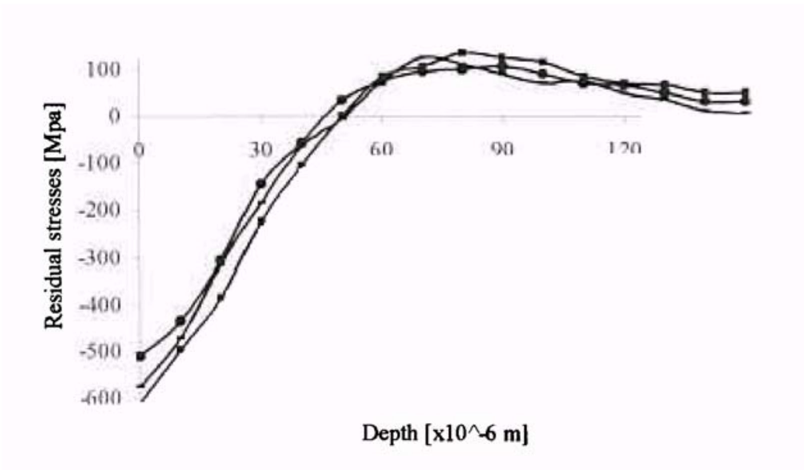

Figure. 7. The residual stresses (σ_{11}) depth profiles induced by high-speed mechanical polishing in HAS 1, HAS 2 and HAS 3 steel marks (• - SI; ■ - S2; ─ - S3)

From 50 μm depth to about 120 μm the stresses become positive and reach a maximum level of about 100 MPa at 70 - 90 μm depth. Under 140 - 150 μm depth the microstresses relax to about zero level.

From our measurement result that the HAS l steel is less distorted by polishing in both cases then HAS 2 and HAS 3 steels i.e. low-speed and high-speed mechanical polishing.

As we expected the vibrational-polishing induced the lowest microstresses in all investigated steel marks as it is shown in Figure 8.

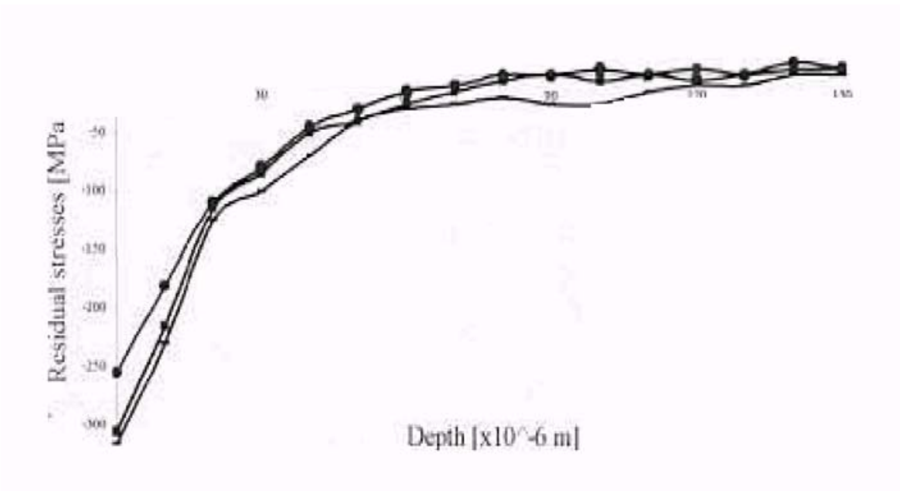

Figure. 8. The residual stresses (σ_{11}) depth profile induced by vibrational-polishing in S1, S2 and S3 steel marks (• - SI; ■ - S2; ─ - S3)

The lowest absolute σ_{11} values induced by high speed-vibration contact polishing can be explained by vibrational stress releasing. The releasing effect can be considered as being at the bulk level because the microstresses attend the zero level at about 60μm depth.

The differences between depth profiles of the HAS1, HAS 2 and HAS3 steels can be related to their structure and from technological point of view they are very important. So, it is demonstrated that mechanical polishing induced high residual microstresses and one of the ways to minimize their intensity is to use vibrational contact polishing technique.

5. Conclusions

The residual stresses induced by milling are quite different from those induced by mechanical polishing. In all cases the HAS 1 steels have better residual stresses states than HAS 2 and HAS S3 steels. It was shown that the high speed-vibrational contact polishing is the best technique for steels of AISI 316 type. The same, the HAS1 steel is the best from the residual stresses point of view.

Symbols and abbreviations

B	Integral width of the (211) lines	[rad]
B_o	The etalon width of the same line	[rad]
E	Young's modulus	[GPa]
υ	Poisson's ratio	[-]
θ	Bragg angle of the X-ray diffraction lines	$[^0]$
λ	X-ray wavelength	[Å]
σ_{II}	Stresses of the second kind or second order	[MPa]
WAXD	Wide Angle X-ray Diffraction	-
HAS	High Alloyed Steel	-

References

[1] Gheorghies, C., Berea, N., The influence of residual stresses on mechanical properties of low carbon steels. *Construction of Machine*, 10-12, 1990.
[2] Guinier, A., *Theorie et technique de la radiocristalografie*. Dunod, Paris, 1966
[3] Pencea, I., *Basics of materials' structural analysis*, Ed. Printech, 2002.
[4] Rasul, I.T., Meguid, S.A., Machining residual stresses, *Mat. Sci and Technol*, 12, 445, 1996.
[5] Bally, D., Benes, L., Manaila, R., *X-ray and Neutron Diffraction*. Technica, 1972.
[6] Pencea, I., *Elements of applied structural analysis*, Ed. Printech, 2002.
[7] Sfat, E.C., *Traitements thermiques des aciers*, Man-Dely Edition, Bucharest, 2004.
[8] Kim, Y.C., Fuji, A., North, T.H., Residual stress and plastic strain in AISI 304L stainless steel, *Mat. Sci. and Technol*, 11, 383, 1995.

Manuscript received: 12.05.2009 / accepted: 30.09.2009